ON THE APPLICABILITY OF DIFFERENT METHODS OF XRD LINE PROFILES ANALYSIS IN ESTIMATING GRAIN SIZE AND MICROSTRAIN IN TUNGSTEN THIN FILMS

IGOR DJERDJ[a,1] ANĐELKA TONEJC[a], ANTUN TONEJC[a] and NIKOLA RADIĆ[b]

[a]Departemnt of Physics, Faculty of Science, University of Zagreb, Bijenička 32, P. O. Box 331, HR-10002 Zagreb, Croatia

[b]Ruđer Bošković Institute, Bijenička c. 54, P.O.Box 180, HR-10002, Zagreb, Croatia

Dedicated to the memory of Professor Zvonko Ogorelec

Different methods of X-ray diffraction line profile analysis (XRDLPA) are used to study microstructural parameters such as crystallite size (diffracted domain size), microstrain and texture in tungsten thin films deposited on glass by DC magnetron sputtering at different substrate temperatures and at different working-gas pressures. The whole-pattern analysis within the Rietveld method, the "single-line" method and "double Voigt" method (equivalent to the Warren-Averbach method) are applied and mutually compared. In addition, the results obtained by the Scherrer method are also discussed. The line broadening has been found to be isotropic, supporting the reliability of usage of the Rietveld method in the size-microstrain extraction.

1. Introduction

Physical properties of nano- and submicro-crystalline materials are an attractive object of study for research and industry development, because they manifest themselves in enhanced mechanical, magnetic or transport properties in the nanocrystalline state. Since the deviation from conventional behaviour is sensitive on crystallite-size and microstrain, when comparing nanocrystalline materials with

---

[1]Corresponding author. Tel.: +385-1-4605530; Fax: +385-1-4680336; E-mail address: idjerdj@phy.hr

conventional materials, one must have a reliable method for measuring them. Numerous methods have been established to extract the grain size and microstrain using XRD line profile analysis. The results are often reasonable and consistent. However, there are also cases in which the results deviate when different methods are applied on the same sample. Depending on the materials under investigation, the authors tried to find the best method for specific cases. For example, Jiang et al. [1] employed the Scherrer equation, integral breadth analysis, and single line approximation to extract grain size and microstrain in Fe-3 wt.% Al alloy powders prepared by different techniques: cryomilling, cold pressing, hot pressing and hot isostatic pressing. They concluded that all employed methods seem to be effective in estimating grain size and microstrain. Vives et al. [2] utilized the Williamson-Hall plot, the Scherrer method, the Voigt model and the Warren-Averbach method in order to calculate the grain size and the lattice microstrain of iron ball-milled powders. However, they found that more accurate results are obtained using the Voigt and Warren-Averbach method in comparison to the Williamson-Hall and Scherrer methods. Similarly, Lucks et al. performed XRD line broadening analysis on ball-milled molybdenum powder [3] and found the Warren-Averbach and an alternative Fourier method after van Berkum et al. [4] to be more accurate for the extraction of grain size and microstrain than the Williamson-Hall method, which was also used. Zhang et al. [5] investigated the microstructure of nanocrystalline materials prepared by cryomilling of A1 powders, applying the Warren-Averbach method, integral breadth and the Scherrer method. They pointed out that the appropriateness of an applied line broadening analysis method can be evaluated according to the values of grain size, calculated by this method, which are closest to the TEM measurement. Therefore, they concluded that the integral-breadth method provides the closest estimation to the TEM results, while the grain size determined by the Warren-Averbach method is smaller than the apparent mean size obtained by TEM. Finally, Mukherjee et al. [6] used the Williamson-Hall plot, the simplified breadth method, and the modified Rietveld method to study microstructural parameters of the heavily deformed solid polycrystalline Zircaloy-2 and Zr-2.5% Nb alloys. They found that the modified Rietveld method is the most suitable method for analyzing the microstructure of these deformed solid samples.

To our knowledge, no such comparative analysis was performed on thin films. In a recent paper [7], we analyzed thin tungsten films that were deposited onto glass substrates by DC magnetron sputtering using the Rietveld method to determine the diffracting domain size and the root-mean-square (r.m.s.) microstrain. In this paper, the size-microstrain analysis is performed using the Rietveld method, the "single-line" method, the Scherrer method and the "double-Voigt" method and the obtained results compared are. Moreover, the preferred orientation effect present in tungsten thin films is thoroughly analyzed.

2. Experimental

Thin tungsten films were prepared in a sputtering system with two cylindrical magnetrons, equipped with a diffusion pump and an auxiliary titanium sublimation

pump, as described earlier [7, 8]. The tungsten films were deposited at substrate temperatures: 77 K, 293 K and 523 K. The working gas pressure was in the range from 0.7 to 2.8 Pa. X-ray diffraction patterns of the studied samples were taken at room temperature using a Philips powder diffractometer (PW 1820) with monochromatized CuKα radiation. The intensity was registered in the angular range of $7° \leq \theta \leq 80°$. NIST SRM 660a LaB$_6$ powdered sample was used as the instrumental standard, and its diffraction pattern was taken under the same conditions as those of tungsten thin films. This was necessary in order to make corrections due to the instrumental broadening of diffraction lines.

3. Line profile analysis methods

The recorded XRD patterns of investigated tungsten thin films were subsequently refined by the Rietveld method [9] using the program FULLPROF [10]. The stable structure of tungsten is body-centered-cubic (bcc α-W). However, a metastable form of A-15 tungsten (β-W) also appeared in thin films [11, 12]. Thus the structures were refined in the space groups of α-W, *Im-3m* and β-W, *Pm-3n*. The refinement sequence was performed first with the scale factors only, increasing the number of refined parameters at each following step. The parameter turn-on sequence in the next runs was: background coefficients, the zero point of the detector, the lattice parameters, the Gaussian, U, V, W and Lorentzian, X, Y halfwidth parameters, the preferred orientation parameters and Debye-Waller parameters. The convergence criterion of iteration process was chosen according to the type of incident radiation. For the case of X-rays (standard θ:2θ diffractometer), the refinement was continued until the shifts in any parameter, Δx_i, were less than one third of its estimated standard deviation, σ_i. The background was taken to be the polynomial function of 2θ of the 3$^{\text{rd}}$ order, because the best fit was obtained only in that case. The size-microstrain analysis in this work was done using three different methods: (a) whole-pattern analysis within the Rietveld method, (b) individual profile line analysis (the "single-line" method), and (c) the "double Voigt" method [13], which is equivalent to the Warren-Averbach method. The well-known Scherrer method, which gives a relatively good estimate of volume-weighted apparent domain size, was also used in the analysis.

3.1. The Rietveld method

In order to make the size-microstrain analysis within the Rietveld method, the chosen diffraction profile function was the modified Thompson-Cox-Hastings pseudo-Voigt [14], with a Lorentzian for size and a Gaussian for microstrain. The extraction of size and microstrain data was performed according to the procedure described in Chapter 8.4 of Ref. [15]. The instrumental line broadening was removed by the deconvolution operation. Application of the Rietveld procedure onto LaB$_6$ (using the same profile function) yields the separation of the Gaussian β_{gG} and Lorentzian β_{gL} integral breadth components of instrumental profile. The re-

fined values of halfwidth parameters, $U = 0.006$, $V = -0.01234$, $W = 0.0062$, $X = 0.01419$, $Y = 0.07306$, define β_{gG} and β_{gL} through the following equations

$$\beta_{gG}^2 = \frac{\pi}{4\ln 2}(U\tan^2\theta + V\tan\theta + W)\,, \tag{1}$$

$$\beta_{gL} = \frac{\pi}{2}\left(X\tan\theta + \frac{Y}{\cos\theta}\right)\,. \tag{2}$$

Afterwards, the similar procedure was then applied to the experimental profile $h(x)$, but this time keeping the parameters V, W and X at instrumental values and varying only parameters U and Y. The obtained integral breadth values β_{hG} and β_{hL} are then converted to the integral breadth values β_{fG} and β_{fL} of deconvoluted sample profile $f(x)$ using Eqs. (3) and (4)

$$\beta_{fL} = \beta_{hL} - \beta_{gL}\,, \tag{3}$$

$$\beta_{fG}^2 = \beta_{hG}^2 - \beta_{gG}^2\,. \tag{4}$$

The obtained integral breadth values of the deconvoluted sample profile $f(x)$ are then converted to the volume-averaged domain (crystallite) size $\langle D_{hkl}\rangle_V$ and r.m.s. microstrain $\langle\varepsilon_{hkl}^2\rangle^{1/2}$ for every hkl reflection using Eqs. (5) and (6) [16],

$$\langle D_{hkl}\rangle_V = \frac{\lambda}{\beta_{fL}\cos\theta}\,, \tag{5}$$

$$\langle\varepsilon_{hkl}^2\rangle^{1/2} = \frac{1}{2\sqrt{2\pi}}\beta_{fG}\,\mathrm{ctg}\,\theta\,, \tag{6}$$

where λ is the wavelength of the X-rays and θ is the Bragg angle.

The previously described procedure results in calculated values of domain sizes and microstrain for each hkl reflection. In this way, we are able to compare domain size values or microstrain values obtained by different XRDLPA methods for each hkl.

3.2. The "single-line" method

The "single-line" method was applied to the selected well-defined non-overlapped diffraction maxima, assuming a Voigtian profile function. The term "well-defined diffraction maximum" here means the diffraction profile line which can be resolved from its background. In this case no structure model is needed. Only a least-squares fitting of the observed diffraction profile to the Voigt function was performed, resulting in the calculated values of the fitting parameters β_{fG} and β_{fL}. Those values yield to the volume-averaged domain (crystallite) size $\langle D_{hkl}\rangle_V$ and r.m.s. microstrain $\langle\varepsilon_{hkl}^2\rangle^{1/2}$ according to the same procedure as in the Rietveld case.

3.3. "Double Voigt" method (Warren-Averbach method)

Previously described methods of size-microstrain analysis are based on a single-line approach. In a case when multiple (at least two) orders of a reflection are available, one can separate the effect of size and microstrain on the line broadening using the Warren-Averbach method [17]. The basis of this method is a separation of effects of crystallite size and microstrain on the line broadening by decomposing the cosine Fourier coefficient A_L of the profile into the product of the size coefficient A_L^S and the microstrain coefficient A_L^D. Fitting the diffraction peaks by the appropriate function allows the calculation of Fourier coefficients A_L^S and A_L^D. In the "double Voigt" method, Balzar and Ledbetter [18] assumed that both the crystallite size and the microstrain broadening are described by the Voigt function. Since the convolution of two Voigt functions is also a Voigt function, according to the characteristics of Gaussian β_G and Lorentzian β_L integral breadths (Eqs. (3) and (4)), one can write the following relations for the resultant integral breadths $\beta_{G,L}$

$$\beta_L = \beta_{LS} + \beta_{LD}\frac{s^2}{s_0^2}\,, \tag{7}$$

$$\beta_G^2 = \beta_{GS}^2 + \beta_{GD}^2\frac{s^2}{s_0^2}\,, \tag{8}$$

where β_S are integral breadths attributed to the crystallite size effect and β_D are integral breadths attributed to the microstrain, s being a variable in reciprocal space. In order to resolve the system of relations (7–8) and calculate the values of β_{LS}, β_{GS}, β_{LD} and β_{GD}, we must know the integral breadths of at least two orders of reflection with reciprocal coordinates s_0 and s. Then the Fourier coefficients of size A^S and microstrain A^D are

$$A^S(L) = \exp(-2L\beta_{LS} - \pi L^2\beta_{GS})\,, \tag{9}$$

$$A^D(L) = \exp(-2L\beta_{LD} - \pi L^2\beta_{GD})\,, \tag{10}$$

where L is the Fourier length, defined according to [17]. From the calculated integral breadths, β_{LS}, β_{GS}, β_{LD} and β_{GD}, one can calculate the characteristic size and microstrain parameters

-the volume-weighted domain size $\langle D\rangle_V$,

$$\langle D\rangle_V = \frac{\exp(k^2)}{\beta_{GS}}[1 - \mathrm{erf}(k)]\,, \tag{11}$$

where $k = \beta_{LS}/(\sqrt{\pi}\,\beta_{GS})$ is the characteristic ratio of integral breadths of the Voigt function, and $\mathrm{erf}(k) = (2/\sqrt{\pi})\int_0^k \mathrm{e}^{-u^2}\,\mathrm{d}u$ is the error function;

-the root mean square microstrain $\langle \varepsilon^2 \rangle^{1/2}$,

$$\langle \varepsilon^2(L) \rangle^{1/2} = \frac{1}{s_0} \left[\frac{\beta_{GD}^2}{2\pi} + \frac{\beta_{LD}}{L\pi^2} \right]^{1/2} . \tag{12}$$

The last expression is in fact the r.m.s. microstrain weighted along the length L. In the calculation procedure, the weighting was taken along the length $L = \langle D \rangle / 2$. In this work, the "double Voigt" method was applied to the diffraction line pair (200)–(400) of β-tungsten using the computer program BREADTH [19]. The input parameters for program BREADTH, β_G, β_L, were taken over output file of the Rietveld program FULLPROF, considering them as integral breadths of two deconvoluted sample broadened diffraction-line profiles. The deconvolution procedure was therefore performed within the program FULLPROF in the same way as described in paragraph 3.1.

3.4. Scherrer method

Finally, using the Scherrer equation, the apparent volume-weighted domain size $\langle D_{hkl} \rangle_V$ was calculated according to

$$\langle D_{hkl} \rangle_V = \frac{K\lambda}{H \cos\theta} , \tag{13}$$

where K is a constant approximately equal to unity and related to the crystallite shape, and H corresponds to the full width at half maximum of the peak.

4. Results and discussion

Figure 1 shows the XRD patterns of the tungsten thin films deposited at room temperature and working-gas pressures of 1.4 Pa and 2.8 Pa. In both samples α-W and β-W are present and their diffraction lines are marked. Several features concerning XRD pattern can be noticed: (i) The intensity of diffraction lines varies from sample to sample, reflecting a different amount of crystalline phases. The tungsten thin film deposited at 1.4 Pa shows a larger amount of α-W in comparison to β-W, while in the sample deposited at 2.8 Pa the composition is reversed, α-W is present in traces. (ii) The diffraction lines are broadened, possibly due to the presence of small grain size (below 100 nm) and/or lattice microstrain. (iii) The stronger intensity of some diffraction lines indicates the presence of texture (preferred orientation), often observed in thin solid films.
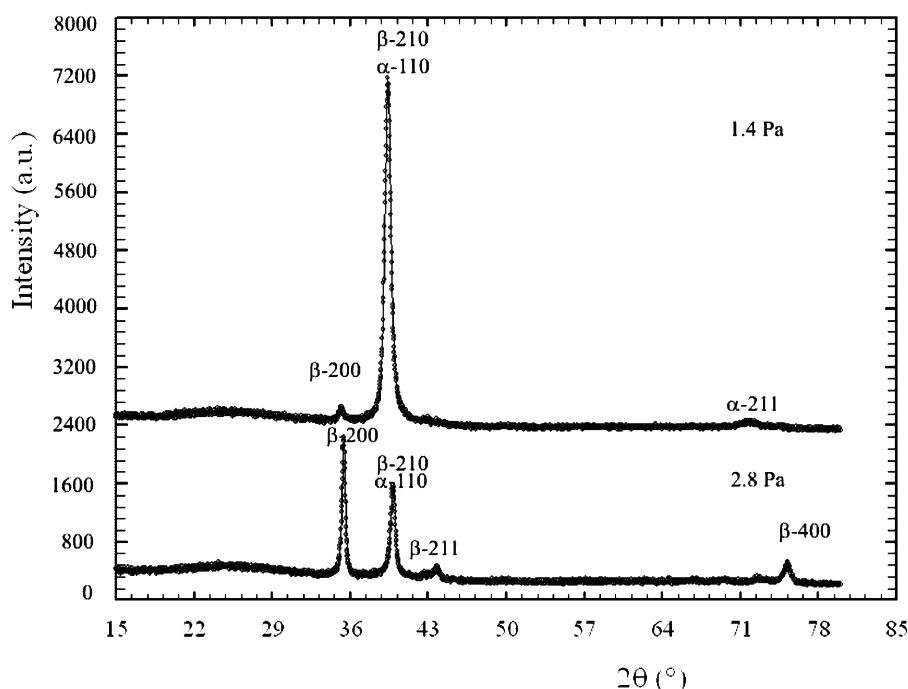
Fig. 1. XRD patterns of tungsten thin film deposited at 1.4 Pa *and 2.8* Pa.

4.1. Correction for the preferred orientation

If the polycrystalline sample shows the preferred orientation, the observed intensity of diffraction pattern also depends on this effect, and can no longer be directly related to the structural parameters. Therefore, the preferred orientation effect should be corrected in order to obtain correct values of structural parameters. Figure 2 shows the plot of the Rietveld refinement of tungsten thin film prepared at Ar pressure of 1.4 Pa and substrate temperature of 77 K. The agreement between the observed and the calculated patterns is poor due to the preferred orientation effect. The calculated peak heights of α-110 and β-200 are underestimated in comparison to the experimental ones, indicating preferred orientation of the α phase along $\langle 110 \rangle$ and preferred orientation of the β phase along $\langle 200 \rangle$ perpendicular to the substrate surface. The same finding of preferred orientation direction was reported elsewhere [20]. In order to correct for the preferred orientation effect, we applied the two-parameter exponential function [15]

$$P_K = G_2 + (1 - G_2)\exp(-G_1\alpha_K^2),\qquad(14)$$

where G_1 and G_2 are refinable parameters and α_K is the acute angle between the preferred orientation direction ($\langle 110 \rangle$ in the case of the α phase and $\langle 200 \rangle$ in the case
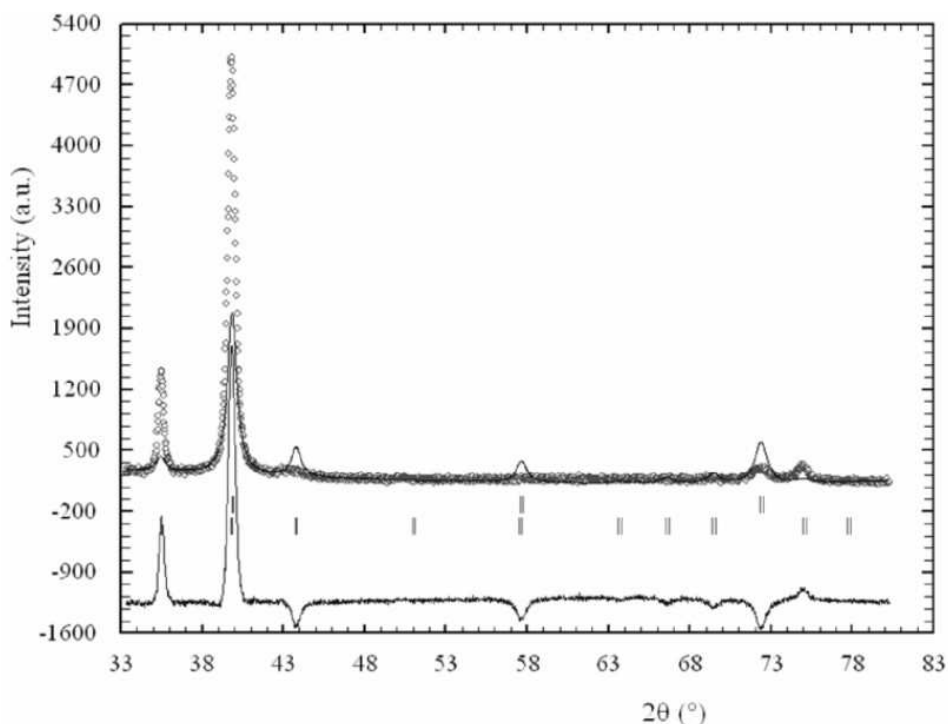
Fig. 2. The structural refinement patterns of thin tungsten film deposited at 1.4 Pa and 77 K without correcting for the preferred orientation effect. The empty circles represent the observed intensities and the solid line represents the calculated ones. The difference (obs.-calc.) is shown beneath. Vertical bars are the reflection position markers, upper row α-W, lower row β-W.

of the β phase) and scattering vector. The parameter G_1 stands for the degree of the preferred orientation, and the parameter G_2 stands for the fraction of the sample that is not textured [10]. The values of parameter G_2 lie in the range from 0 to 1; in the case of value 0, the non-exponential term in Eq. (14) vanishes, implying that the sample is completely (100 %) textured. If the value of G_2 is 1, the exponential term in (14) vanishes, resulting that there is no preferred orientation at all (sample is not textured). By including the preferred orientation effect into the refinement, the calculated peak intensities of all reflections, particularly of β-200 and α-110, were almost identical with the ones at the observed diffraction pattern as shown in Fig. 3. Our results indicate the suitability of correction for the preferred orientation effect by the exponential function in the case of tungsten thin films showing the biaxial preferred orientation effect. The value of refined the parameter G_2 was 0 in the refinement of all XRD patterns, which indicates that the samples were 100% textured. The calculated values of the parameter G_1 have shown different degrees of preferred orientation depending on deposition conditions. These dependences are shown in Fig. 4. One can notice a strong dependence of the parameter G_1 on the
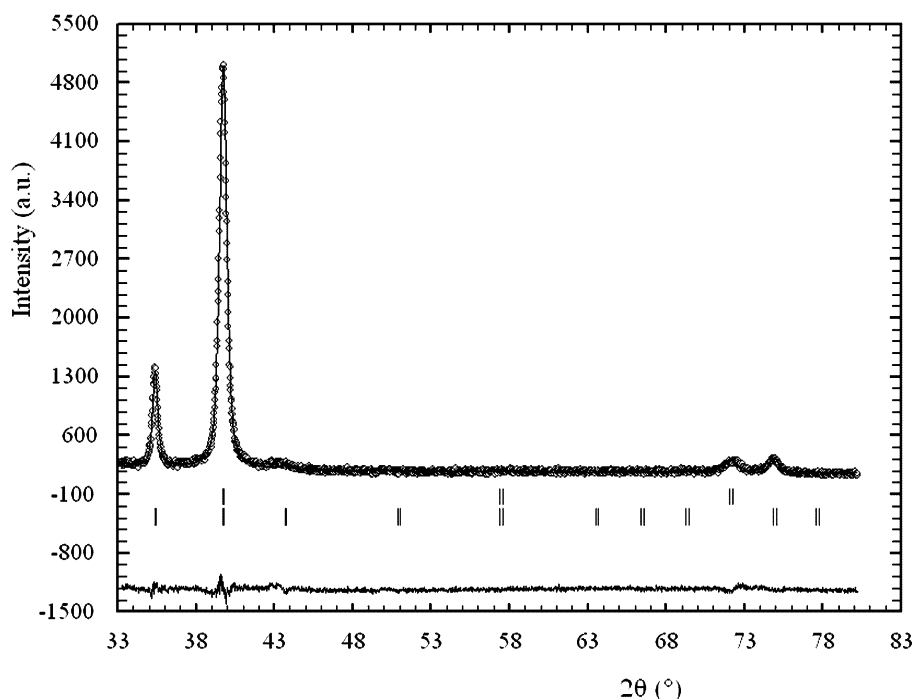
42

Fig. 3. *The structural refinement patterns of thin tungsten film deposited at 1.4 Pa and 77 K after correcting for the preferred orientation effect. The empty circles represent the observed intensities and the solid line represents the calculated ones. The difference (obs.-calc.) is shown beneath. Vertical bars are the reflection position markers, upper row α-W, lower row β-W.*
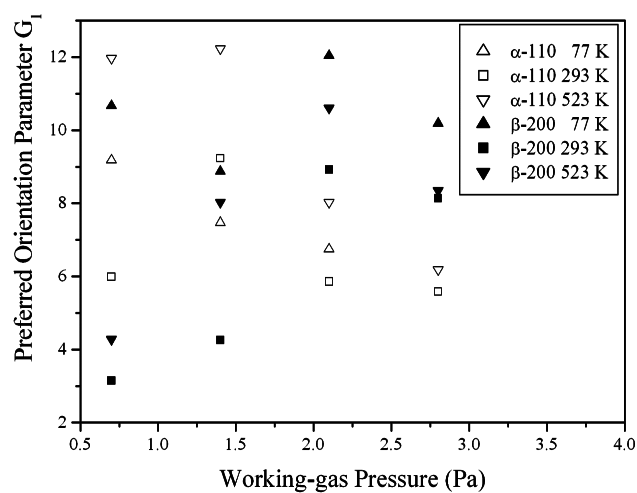

Fig. 4. *Dependence of the α-110 and β-200 preferred orientation parameter G_1 on the working-gas pressure and substrate temperature.*

substrate temperature for both phases. In the case of α-110, the parameter G_1 is decreasing in this substrate temperature sequence: 523 K > 77 K > 293 K. The exception to this rule is for the pressure of 1.4 Pa, where the sample deposited at 293 K shows stronger preferred orientation than the sample deposited at 77 K. In the case of β-200 preferred orientation, parameter G_1 is decreasing in this substrate temperature sequence: 77 K > 523 K > 293 K. In both cases, the minimum of preferred orientation is achieved for films deposited onto the substrate at room temperature. Regarding the dependence of the parameter G_1 on Ar pressure, no regularity has been observed.

4.2. Rietveld and "single-line" profile methods

The results of size-microstrain analysis, volume averaged grain size $\langle D \rangle_V$ and r.m.s. microstrain $\langle \varepsilon^2 \rangle^{1/2}$ obtained by described methods are presented in Table 1. By inspecting the table, one can see that some values of domain size and r.m.s. microstrain within the Rietveld method column are not given. This is the consequence of the failure of the Rietveld method, due to the low intensity of the diffraction lines needed for comparison with others within the same XRD pattern. Moreover, in some cases the intensities of those diffraction lines are comparable to the background, which is an additional difficulty in extracting size-microstrain by the Rietveld method. To overcome those problems and to extract size-microstrain values of those lines, too, the "single-line" method, based on a fitting of isolated diffraction line profiles by the Voigt function, was adopted. As already mentioned in Sect. 3, this method is applied not only to the lines where the Rietveld method has failed, but also to all other well-defined non-overlapped diffraction lines (Table 1). An example of a fit of the isolated β-200 diffraction peak by the Voigt function is presented in Fig. 5. The results of single-line method are displayed in columns 7 and 8 of Table 1. Grain size and microstrain values calculated by this method are larger
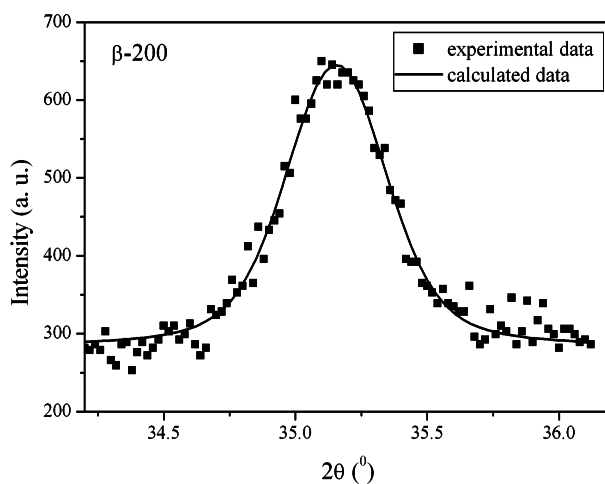

Fig. 5. Fit with a Voigt function of the β-200 reflection.

TABLE 1. Results for the volume-weighted average grain size $\langle D \rangle_V$ and r.m.s. microstrain $\langle \varepsilon^2 \rangle^{1/2}$ calculated using different line profile analysis methods for different hkl reflections, and samples deposited at different Ar pressures and substrate temperatures.

$T_{\text{substrate}}$ (K)	p_{Ar} (Pa)	Phase	hkl	Rietveld method $\langle D \rangle_V$ (nm)	$\sqrt{\langle \varepsilon^2 \rangle}$ (%)	Single line method $\langle D \rangle_V$ (nm)	$\sqrt{\langle \varepsilon^2 \rangle}$ (%)	Scherrer method $\langle D \rangle_V$ (nm)	W–A 200–400 $\langle D \rangle_V$ (nm)	$\sqrt{\langle \varepsilon^2 \rangle}$ (%)
77	0.7	α	110	19.2	0.397				33.5	0.353
		α	211	19.1	0.394	6.6	0.238	10		
		β	200	46.7	0.377	60.8	0.345	39		
		β	210	46.5	0.375					
		β	400	45.1	0.322	16.9	0.291	15		
77	1.4	α	110	19.2	0.348				22.1	0.265
		α	211	18.9	0.345	14.9	0.437	10		
		β	200	25.3	0.270	37.8	0.287	40		
		β	210	25.3	0.268					
		β	400	24.9	0.263	14.7	0.208	16		
77	2.1	α	110	15.9	0.318				31.6	0.202
		α	211	15.7	0.314	12.7	0.248	1		
		β	200	39.5	0.210	65.7	0.229	60		
		β	210	39.3	0.207					
		β	400	38.3	0.201	27.6	0.169	27		
77	2.8	β	200	26.9	0.266	40.9	0.264	38	23.3	0.260
		β	210	26.9	0.264					
		β	400	26.4	0.259	16.3	0.210	17		
293	0.7	α	110	13.6	0.393			8		
		α	211	13.5	0.389			5		
		β	200			31.7	0.402	43		
293	1.4	α	110	16.5	0.402					
		α	211	16.3	0.398	9.3	0.616	6		
		β	200			17.7	0.292	34		
293	2.1	α	110	13.2	0.243				20.0	0.105
		α	211	13.1	0.237	7.4	0.276	9		
		β	200	25.7	0.178	52.1	0.254	51		
		β	210	25.6	0.174					
		β	400	25.2	0.167	49.5	0.198	36		
293	2.8	β	200	23.9	0.266	38.8	0.253	40	21	0.262
		β	210	23.8	0.263					
		β	211	23.8	0.262					
		β	400	23.4	0.259	15.9	0.151	19		
523	0.7	α	110	11.8	0.338					
		α	211	11.7	0.334					
		β	200			60.8	0.414	34		
		β	400					14		
523	1.4	α	110	16.4	0.359				16.6	0.262
		α	211	16.3	0.355			5		
		β	200	18.2	0.257	24.1	0.234	38		
		β	210	18.2	0.254					
		β	400	17.9	0.249	35.9	0.338	15		
523	2.1	α	110	15.4	0.363				26.3	0.207
		α	211	15.2	0.360	6.8	0.325	8		
		β	200	31.0	0.211	47.3	0.235	51		
		β	210	30.9	0.208					
		β	400	30.3	0.202	24.6	0.190	25		
523	2.8	α	110	11.5	0.328				28.3	0.202
		α	211	11.5	0.324			7		
		β	200	34.2	0.227	54.9	0.246	52		
		β	210	34.1	0.224					
		β	400	33.3	0.218	27.8	0.221	24		

in the low-angle range. For example, for the sample deposited at 293 K and 2.8 Pa, the average grain size calculated from the 200 diffraction maximum of β-W is 38.8 nm and the corresponding microstrain is 0.253%. However, the calculation of the same quantities for the 400 peak yields the values which are about a half of the values calculated from the 200 peak, 15.9 nm and 0.151%. The only exception to this observed behaviour is the sample deposited at 523 K and 1.4 Pa, where the opposite holds. The results of size-microstrain analysis obtained by the single-line method suggest the anisotropic character of the diffraction line broadening. However, the comparison of grain size and microstrain values belonging to the different *hkl* but the same phase calculated by the Rietveld method shows high isotropic broadening. To remove doubts whether the broadening is isotropic or anisotropic, we plotted the variation of the full width at half maximum (FWHM) with diffraction angle 2θ. This variation is shown in Fig. 6 for β-W calculated from the XRD pattern of tungsten film deposited at 293 K and 2.8 Pa. Since the FWHM of selected peaks varies smoothly with a scatter variable, the contribution of microstructural effects is isotropic [15]. Moreover, almost linear dependence was observed and marked by a straight line in Fig. 6.
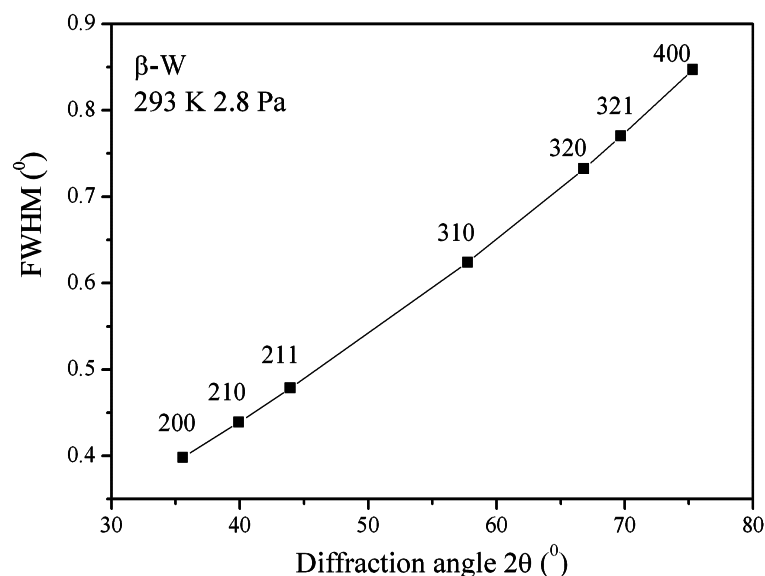

Fig. 6. Variation of full width at half maximum (FWHM) with 2θ for observed hkl diffraction lines of β-W prepared at 293 K and 2.8 Pa.

4.3. The Scherrer method compared to other methods

When the peak broadening is attributed to the sole effect of the diffracting domain size, the Scherrer method is applicable. However, if microstrain is present, then the Scherrer method could serve as a rough estimate of average volume-

weighted domain size. The results of the Scherrer method are given in column 9 of Table 1, for comparison with the sizes obtained using other methods. In the case of β-W among the selected 200 and 400 peaks, the larger grain size is always found to correspond to the 200 peak, since the contribution of the microstrain effect to the peak broadening is comparatively small in the low-angle range. The same holds for α-W, however that is only obvious for a sample prepared at 293 K and 0.7 Pa, where the amount of α-W is high and many diffraction lines of α-W are observed. Similarly, as in the case of the single-line method, the different values of the grain size for the same phase but different hkl indicate the apparent anisotropic broadening.

4.4. Discussion of the applicability of XRDLPA methods

The average volume-weighted domain size $\langle D \rangle_V$ and r.m.s. microstrain $\langle \varepsilon^2(L) \rangle^{1/2}$ calculated by the "double-Voigt" method (consistent with the Warren-Averbach formalism) are summarized in the last two columns of Table 1 for a β phase. The results obtained by this method are then related to the direction normal to one family of planes, here the {200} planes.

By analyzing the obtained results of size-microstrain summarized in Table 1, one can see that the average volume-weighted domain sizes of β-W are larger in comparison to α-W within the same sample. Similarly, the r.m.s. microstrain values of β-W are a bit smaller in comparison to α-W. For example, for a tungsten thin film deposited at Ar pressure of 0.7 Pa and substrate temperature of 77 K, average volume-weighted domain size of β-200, $\langle D_{\beta-200} \rangle_V = 46.7$ nm, which is significantly larger than the domain size of α-110, $\langle D_{\alpha-110} \rangle_V = 19.2$ nm. For the same sample, the r.m.s. microstrain value of the β phase, $\langle \varepsilon_{\beta-200}^2 \rangle^{1/2} = 0.377\%$, is slightly lower than the r.m.s. microstrain value of the α phase, $\langle \varepsilon_{\alpha-110}^2 \rangle^{1/2} = 0.397\%$.

The plots of the average volume-weighted domain size $\langle D \rangle_V$ and r.m.s. microstrain $\langle \varepsilon^2 \rangle^{1/2}$ calculated by employed line broadening methods as a function of the working-gas pressure for β-200 are shown in Figs. 7a and b, respectively. It must be stressed that, in Fig. 7a, the highest value of grain size is obtained by the single-line method and the lowest one by the "double-Voigt" method. In a microstrain case, Fig. 7b, the lowest values are also obtained by the "double-Voigt" method. Figure 7a illustrates a slight discrepancy in the grain sizes obtained by different methods. Similar findings are reported elsewhere [1, 2]. Figure 7b shows a fairly good agreement among microstrain values obtained by different methods.

Among the XRDLPA methods, the "double-Voigt" method should give the most reliable data, due to the fact that the size and microstrain, which are two variables, are extracted from two reflections. Contrary to that, in the "single-line and Rietveld methods the size and microstrain are calculated from one reflection [21]. Therefore, their use results in less reliable size and microstrain values in comparison to the "double-Voigt". By carefully inspecting Fig. 7a, it can be seen that more homogeneous results in grain size analysis are obtained comparing either the Rietveld
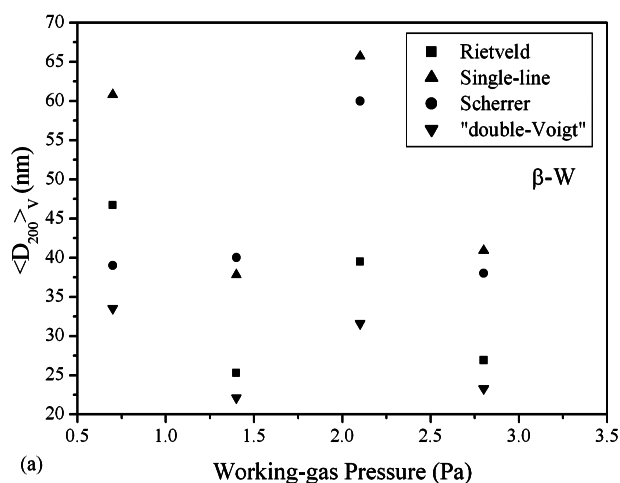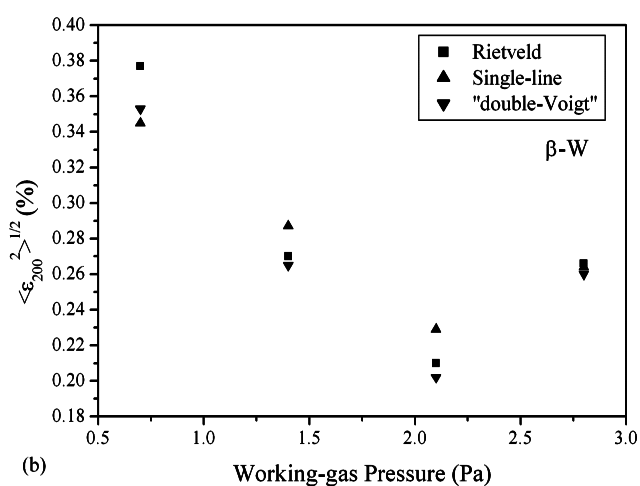
Fig. 7. a) Evolution of average volume-weighted domain size of β tungsten $\langle D_{200}\rangle_V$ with working-gas pressure obtained with different line profile analysis methods; (b) Evolution of r.m.s. microstrain $\langle\varepsilon_{200}^2\rangle^{1/2}$ of β tungsten with working-gas pressure obtained with different line profile analysis methods.

and "double-Voigt methods or the Scherrer and single-line methods than comparing all methods. The exception of this finding is sample deposited at working-gas pressure of 0.7 Pa.

In the case of microstrain (Fig. 7b), closer values are achieved using the Rietveld and "double-Voigt" methods. If we take into account that line broadening is isotropic, which was supported by the almost linear graph shown in Fig. 6, the correct result of size-microstrain analysis is obtained with the Rietveld and "double-Voigt" methods. Moreover, the Rietveld method gave quantitative information of the microstructural parameters considering all diffraction peaks, contrary to the single-line or Scherrer methods.

Hence, we have found that the Rietveld and "double-Voigt" methods are the most suitable methods for analyzing the microstructure of tungsten thin films.

5. *Conclusion*

The microstructure of tungsten thin films deposited under different conditions was reliably estimated by the XRDLPA using different model-based approaches. The volume-weighted average grain size and r.m.s. microstrain were calculated. The analysis revealed that the microstructural broadening varies smoothly along different crystallographic directions, indicating a clear signature of isotropy. All applied XRDLPA methods displayed larger grain sizes and smaller r.m.s. microstrain of the β phase in comparison to the α phase. The Scherrer method has to be employed only as a first qualitative approximation, while more accurate results are obtained using the "double Voigt" (Warren-Averbach) and Rietveld methods. In the case of Rietveld method failure, when the intensities of diffraction lines are comparable to the background, the "single-line" method is applicable in size-microstrain extraction, but only as a rough estimate. The Rietveld refinement also revealed that the crystallites of the α phase were preferentially oriented along the $\langle 110 \rangle$ axis and those of the β phase along the $\langle 200 \rangle$ axis perpendicular to the substrate surface.

Acknowledgements

References

[1] H. G. Jiang, M. Rhle and E. J. Lavernia, J. Mater. Res. **14** (1999) 549.

[2] S. Vives, E. Gaffet and C. Meunier, Mat. Sci. Eng. A **366** (2004) 229.

[3] I. Lucks, P. Lamparter and E. J. Mittemeijer, Mat. Sci. Forum **378–381** (2001) 451.

[4] J. G. M. van Berkum, A. C. Vermeulen, R. Delhez, Th. de Keijser and E. J. Mittemeijer, J. Appl. Cryst. **27** (1994) 345.

[5] Z. Zhang, F. Zhou and E. J. Lavernia, Metallurg. Mat. Trans. A A **34** (2003) 1349.

[6] P. Mukherjee, A. Sarkar, P. Barat, S. K. Bandyopadhyay, P. Sen, S. K. Chattopadhyay, P. Chatterjee, S. K. Chatterjee and M. K. Mitra, Acta Mater. **52** (2004) 5687.

[7] I. Djerdj, A. M. Tonejc, A. Tonejc and N. Radić, Vacuum **80** (2005) 1-3 151.

[8] N. Radić, A. Tonejc, M. Milun, P. Pervan, J. Ivkov and M. Stubičar, Thin Solid Films **317** (1998) 96.

[9] H. M. Rietveld, J. Appl. Cryst. **2** (1969) 65.

[10] J. Rodriguez-Carvajal, *FULLPROF-A program for Rietveld Refinement*, Laboratorie Leon Brillouin, CEA-Saclay, France (2000).

[11] Y. G. Shen and Y. W. Mai, J. Mat. Sci. **36** (2001) 93.

[12] I. C. Noyan, T. M. Shaw and C. C. Goldsmith, J. Appl. Phys. **82** (1997) 4300.

[13] D. Balzar, J. Appl. Cryst. **25** (1992) 559.

[14] P. Thompson, D. E. Cox and J. B. Hastings, J. Appl. Cryst. **20** (1987) 79.

[15] R. A. Young (Ed.), *The Rietveld method*, IUCr Monographs on Crystallography **5**, Oxford University Press, Oxford, UK (1996) p. 132.

[16] Th. De Keijser, E. J. Mittemeijer and H. C. Rozendaal, J. Appl. Cryst. **16** (1983) 309.

[17] B. E. Warren, *X-ray Diffraction*, Addison-Wesley, New York (1969).

[18] D. Balzar and H. Ledbetter, J. Appl. Cryst. **26** (1993) 97.

[19] D. Balzar, *BREADTH-a program for analyzing diffraction line broadening*, J. Appl. Cryst. **28** (1995) 244.

[20] T. J. Vink, W. Walrave, J. L. C. Daams, A. G. Dirks, M. A. J. Somers and K. J. A. van den Aker, J. Appl. Phys. **74** (1993) 988.

[21] Th. de Keijser, J. I. Langford, E. J. Mittemeijer and A. B. P. Vogels, J. Appl. Cryst. **15** (1982) 308.

PRIMJENJIVOST RAZLIČITIH METODA ANALIZE PROFILA LINIJA XRD ZA OCJENJIVANJE VELIČINE ZRNACA I MIKRONAPREZANJA U TANKIM SLOJEVIMA VOLFRAMA

Primijenili smo različite metode za analizu profila linija rendgenske difrakcije radi proučavanja mikrostrukturnih parametara, kao što su veličina kristalita (veličina difrakcijskih domena), mikronaprezanja i struktura u tankim slojevima volframa naparenim na staklo magnetronskim DC raspršivanjem pri različitim temperaturama podloge i radnim tlakovima plina. Primijenili smo cjelovitu analizu spektara Rietveldovom metodom, metodom "jedne linije" i metodom "dvo-Voigta" (jednakovaljanog metodi Warrena-Averbacha) i usporedili ih. Nadalje, raspravljamo i rezultate dobivene Scherrerovom metodom. Nalazimo da je širenje linija izotropno, što potvrđuje pouzdanost primjene Rietveldove metode za izvođenje veličine i mikronaprezanja.